

Behavior of SiC at high temperature under helium with low oxygen partial pressure

J. Eck^a, M. Balat-Pichelin^{a,*}, L. Charpentier^a, E. Bêche^a, F. Audubert^b

^a PROMES-CNRS, 7 rue du four solaire, 66120 Font-Romeu, Odeillo, France

^b DEC/SPUALTEC, Bât. 307, CEA Cadarache, 13108 St Paul lez Durance, France

Received 8 December 2007; received in revised form 11 April 2008; accepted 25 April 2008

Available online 13 June 2008

Abstract

The behavior of SiC at high temperature under helium with low oxygen partial pressure is a key factor for its application as structural material in Gas-cooled Fast Reactors (GFR). After a literature study on the active–passive transition in the oxidation of SiC, a numerical study reproducing environments of the future reactors was realized with GEMINI software to evaluate SiC behavior under helium with low oxygen partial pressure (0.5–3500 Pa). It was found that increasing the partial pressure of oxidant pushes the passive to active transition to higher temperature and suppresses the vaporization of SiC. These results are in agreement with the calculation using the Wagner model. Experimental tests at high temperature (1300–2000 K) on massive SiC samples (sintered α and β CVD), coupled to SEM, XPS and XRD analyses before and after oxidation tests are presented. They show that the level of oxidizing species has an important impact on the physico-chemical behavior of SiC as was also predicted by thermodynamic calculation. In addition, for the mass loss with time, the crystallographic structure is an important factor. Silicon carbide is a promising structural material for Generation IV nuclear reactors. Because of its mechanical and physico-chemical properties, it maintains its structural integrity at high temperature in helium environment with low oxygen partial pressure.

© 2008 Elsevier Ltd. All rights reserved.

Keywords: Surfaces; Corrosion; SiC; Nuclear applications; Oxidation

1. Introduction

The worldwide growth in the demand for energy and electricity, coupled with the decrease of fossil fuel reserves and the increase in concern over global warming issues have resulted in a renewed interest in the development of nuclear energy. Ten countries have agreed on a framework for international cooperation in research for a future generation of nuclear energy systems, known as Generation IV. These systems will provide better economical competitiveness and sustainable energy generation, excel in safety and reliability, and also minimize and manage their nuclear waste, by notably reducing the production of long-lived radioactive isotopes. Of particular interest is the GFR (Gas-cooled Fast Reactor) system, which features a fast-spectrum helium-coolant reactor and closed fuel cycle. The nominal operating temperature of this system is about 1500 K.

The high outlet temperature of the helium coolant and its elevated pressure (7 MPa) make it possible to deliver electricity, hydrogen or heat with high conversion efficiency. As a consequence, the development of very high temperature materials with higher resistance to fast-neutron fluence and enhanced fission product retention capability is of interest. SiC is a promising candidate based on its low activation, its low density and its high temperature mechanical strength and thermal shock resistance.¹

As part of this investigation, a literature study was made to understand the behavior of SiC at high temperature under oxidizing conditions. Then, the impact of different parameters (pressure, temperature, partial pressures of O₂, H₂O...) was modeled using a simulation code and compared to an analytical calculation using the Wagner model² previously adapted to SiC by Balat.^{3,4} Finally, to compare with the theoretical results, an experimental study was conducted using the MESOX facility of the PROMES-CNRS laboratory.

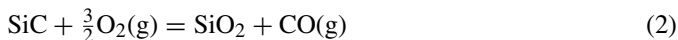
Structural materials for future nuclear reactors should be able to resist very high temperatures, retain their mechanical properties, retain their thermal conductivity and resist fast-neutron

* Corresponding author. Tel.: +33 468 307 768; fax: +33 468 302 940.
E-mail address: marianne.balat@promes.cnrs.fr (M. Balat-Pichelin).

irradiation. SiC is a material that could be used in such extreme conditions, thanks to its physico-chemical properties. In comparison with existing super-alloys, SiC has a lower density and a better resistance to oxidation in the nominal conditions of the reactor.

The oxidation of SiC is of particular interest due to its two different oxidation regimes that depend on its crystallographic form, the total pressure, and the partial pressure of the oxidant in the medium. If the oxidant partial pressure is high enough, the oxidation is passive and a protective, dense and homogenous layer of SiO₂ is formed on the material surface. In contrast, if the oxidant partial pressure is too low, the oxidation is active and a gaseous oxide is formed. In this case, SiC is not protected and loses mass.^{3,4}

Oxygen is the main oxidizing species studied and the following chemical reactions describe the two oxidation regimes of SiC at high temperature, (1) active oxidation and (2) passive oxidation:



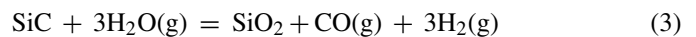
We can find in the critical reviews from Balat⁴ and Presser and Nickel⁵ transitions from passive to active oxidation regime, theoretical or experimental data, according to the partial pressure of oxygen species and the temperatures. The variety of reported experimental results can be explained by the nature of the silicon carbide specimen (polytype, purity, microstructure – grain size, grain boundary density. . . – and composition – impurities or sintering aids contents), the gas flow, the partial and total pressures, the method used and the criterion taken to define the transition. In one of the most recent studies, Ogura and Morimoto⁶ determined experimental transitions on CVD β-SiC under pure oxygen at very low total pressure. In their experiments, high-temperature mass spectrometric analyses were carried out with increasing temperature from 1520 to 1970 K at a rate of 0.75 K s⁻¹ for an oxygen pressure of 0.89, 2.1 and 6.5 Pa. They reported active-to-passive transition according to the rises in ion currents at *m/e* = 28 (CO) and *m/e* = 12 (atomic C). The transition was observed at 1740 K for *p*O₂ = 0.89 Pa, 1790 K for *p*O₂ = 2.1 Pa, and 1920 K for *p*O₂ = 6.5 Pa. But they worked in non-stationary conditions, and the transition might be delayed due to the formation of silica during heating. Narushima et al. also reviewed the literature on passive and active oxidation kinetics.⁷

The present study is done, as in the literature there is no information on the active-to-passive transition under neutral gas at atmospheric total pressure with the very low oxygen partial pressures of interest. In the past, we have already worked on the active-to-passive transition using the Wagner model and experiments were carried on both sintered α-SiC and CVD β-SiC using concentrated solar energy which enables stationary high-temperature conditions with really short periods of heating (a few seconds). The gas (standard air and air plasma), the total pressure and the temperature conditions were different due to the application – atmospheric re-entry of space vehicles.⁴

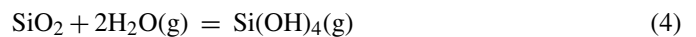
When the reaction products are mainly gaseous, oxygen reacts directly with SiC and the mass loss rate is linear. On

the other hand, if silica is formed, the oxidation rate, after an initial linear regime, becomes parabolic. Parabolic kinetics are justified by the fact that oxygen must diffuse through an outer layer of SiO₂ to react with the substrate. In the same manner, reaction products must diffuse back to the surface to be emitted. Concerning the two regimes, the rate depends on the oxygen partial pressure, which supports the contention that the diffusion of the oxidizing species is the limiting reaction step.^{3,4}

Experimentally, it has been showed that water vapor increases the oxidation rate.^{8–14} Thus, in an atmosphere composed of 50% water vapor and 50% oxygen and for temperatures between 1470 and 1670 K, water vapor is the major oxidizing species, and the reaction is:



Under these conditions, the oxidation rate is proportional to the partial pressure of water vapor, as with oxygen, and is governed by the molecular diffusion through the oxide layer. A consequence of the presence of water vapor is the vaporization of SiO₂ by the reaction (4), with Si(OH)₄ being the primary volatile product, according to¹⁴:



1.1. Case of the GFR

Helium does not chemically react with silicon carbide. However, it is impossible to separate all of the impurities present in the gas. These species could be oxidants like oxygen or water vapor, which are typically present in quantities from 2 to 20 ppm, which can lead to the active oxidation of SiC.¹⁵

One way to thermodynamically solve the stability problem of SiC under helium containing few impurities is to determine a critical temperature for the passive to active oxidation transition, which should be equivalent to a critical temperature for the decomposition for SiO₂ on SiC. For long times, the nominal conditions must be lower than the critical temperature for the passive to active oxidation to ensure the stability of a protective silica layer. In addition, these critical temperatures can vary according to the type of impurity and the total pressure of the medium. Indeed, these values are higher when the oxidizing species is oxygen and lower when it is carbon dioxide¹⁶ or water vapor. These two last impurities tend to decrease the temperature of the passive to active oxidation transition of SiC. The pressure increase influences the stability range of the solid species, by increasing the temperature where their vaporization begins, but also by limiting the outward diffusion of gaseous reaction products, even if the inward diffusion of oxidizing species is increased.

To conclude, the oxidation of SiC at constant temperature and total pressure depends on the partial pressure of the oxidant in the surrounding atmosphere. If the oxygen partial pressure is high enough, a homogenous and protective silica layer can be formed, passive oxidation occurs. In the other case, for low oxygen partial pressures, oxidation is active and the reaction products are mainly gaseous, or the oxide layer is heterogeneous and does not protect the bulk material.

For GFR, which has extreme nominal conditions of use (1500 K, 7 MPa) and uses helium with ppm levels of oxidants, there is no specific study of the silicon carbide behavior in the open literature. Likewise, no more data are found for behavior in accident conditions, where temperatures can reach 2300 K due to depressurization and various gas, oxidizing or not, are added to restore nominal pressure.

2. Numerical study

The software used in this study was developed by ThermoData.¹⁷ Gemini is a code that calculates the thermochemical equilibrium of a system by minimizing its global energy or more exactly its thermodynamic potential. The minimization method used is based on a global optimization technique, adapted to chemical equilibrium.

The potential minimum is searched, taking into account two constraints: mass balance and the quantity of each species must be positive.

Coach is a database management system for Gemini and it is dedicated to the thermochemical properties of the elements and compounds. It contains the overall properties of substances and their reactions. The thermochemical properties always correspond to the substance in its standard state, and are all calculated from basic data of the elements and compounds.

The aim of this simulation is to reproduce the interactions that could occur between SiC and the impurities contained in helium over temperature ($1300 \leq T \leq 2300$ K) and pressure ($P = 10^5$ Pa, 1 and 7 MPa) ranges consistent with the GFR application. According to the gas supplier (Air Liquide), typical impurities in helium are mainly oxygen (20 ppm) and water (5 ppm).

The impurity levels have been varied in the calculations to evaluate their impact on the material as a function of temperature and pressure, allowing for direct comparison with experimental or representative values for the future reactors. However, data (specific heat, enthalpy, entropy, . . .) supplied by the software are determined at standard state, so the results assume that the values of C_p , ΔH_f° , S° , etc. do not vary with pressure. This is normally an accurate approximation for pressures below the GPa level.

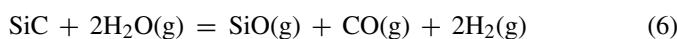
To determine the important parameters in the system, the variance was calculated using the Gibbs' phase rule:

$$V = c + 2 - \varphi \quad (5)$$

where c is the number of independent constituents and φ is the number of phases in equilibrium in the system.

The variance calculation for the system with O_2 as the only oxidant was performed by Balat,^{3,4} leading to a value of 3. So when total pressure and temperature are fixed, the only independent variable is the partial pressure of O_2 .

The variance is then calculated for the system with both O_2 and H_2O in the carrier gas He. In the system He– O_2 – H_2O , there are 9 main significant constituents (α -SiC, SiO_2 , SiO, O_2 , H_2O , CO, H_2 , $Si(OH)_4$ and He) linked by 4 reactions, the (3) and (4) ones and the following (6) and (7):



The number of independent constituents is in fact equal to 5. There are also 3 phases in equilibrium, 2 solids (SiC and SiO_2) and a gaseous mix. Thus the variance of the system can be deduced and is equal to 4, so when total pressure and temperature are fixed, the only influent parameters are both the partial pressures of O_2 and H_2O .

2.1. Results

The calculation was arbitrarily realized with 1 mol of SiC and 1 mol of He and a low content of oxygen varying from 10 to 1000 ppm, the total pressure moving from 0.1 to 7 MPa. Thus, the molar fraction of oxygen was changed and so its partial pressure.

For the He– O_2 system at atmospheric pressure and over the temperature range (1300–2300 K) studied, nearly all of the SiC was preserved (Fig. 1a) for low (10 ppm O_2) impurity levels. SiO_2 is present only at 1300 K (Fig. 1b). Above this temperature, SiC undergoes active oxidation with the formation of SiO and CO from 1400 to 2000 K. Then, for higher temperatures, Si_2C and SiC_2 appear (Fig. 1b).

Increasing the pressure from 10^5 Pa to 7 MPa (Fig. 1c) pushes the stability limit for SiO_2 to higher temperatures (1300 K versus 1500 K). Likewise, increasing the partial pressure of oxygen from 0.5 to 35 Pa, pushes the passive to active oxidation transition to higher temperature. The vaporization of the SiC material is suppressed, as characterized by the quantity of Si_2C and SiC_2 emitted, which is twenty times lower for 7 MPa than for 10^5 Pa. Moreover, the temperature at which SiC vaporization begins is 2200 K for 7 MPa compared to 2000 K for 10^5 Pa (Fig. 1b and c).

The increase of the proportion of oxidizing species by two orders of magnitude allows a silica layer to form at elevated temperatures (Fig. 1c and d). At the nominal temperature and pressure of the reactor, that is to say about 1500 K and 7 MPa, SiC begins to form silica at 10 ppm of oxygen. However, the amount of oxide is probably not enough to protect the SiC. For operating conditions, at 1900 K, the oxygen content has to reach more than 1000 ppm to preserve a silica layer. For accident conditions, near 2300 K, an oxygen concentration of 10^5 ppm is required to stabilize an oxide layer as the thermodynamics predict the vaporization of SiC above 2000 K. However, no study has been reported in the open literature at such temperatures because the limit for use of SiC is about 2000 K, for atmospheric pressure.

Concerning the He– O_2 – H_2O system, O_2 and H_2O species both contribute to silicon carbide oxidation. When present in the same proportions, their effects on the material are different (Fig. 2). For 1000 ppm, the quantity of SiC consumed by the oxidation reaction with O_2 is two times higher than for H_2O as expected from the stoichiometry of the equilibria. On the other hand, the quantity of SiO_2 formed, which is directly related to the amount of SiC consumed, is higher when O_2 is the oxidant. The stability range of silica is also reduced by 100 K when water

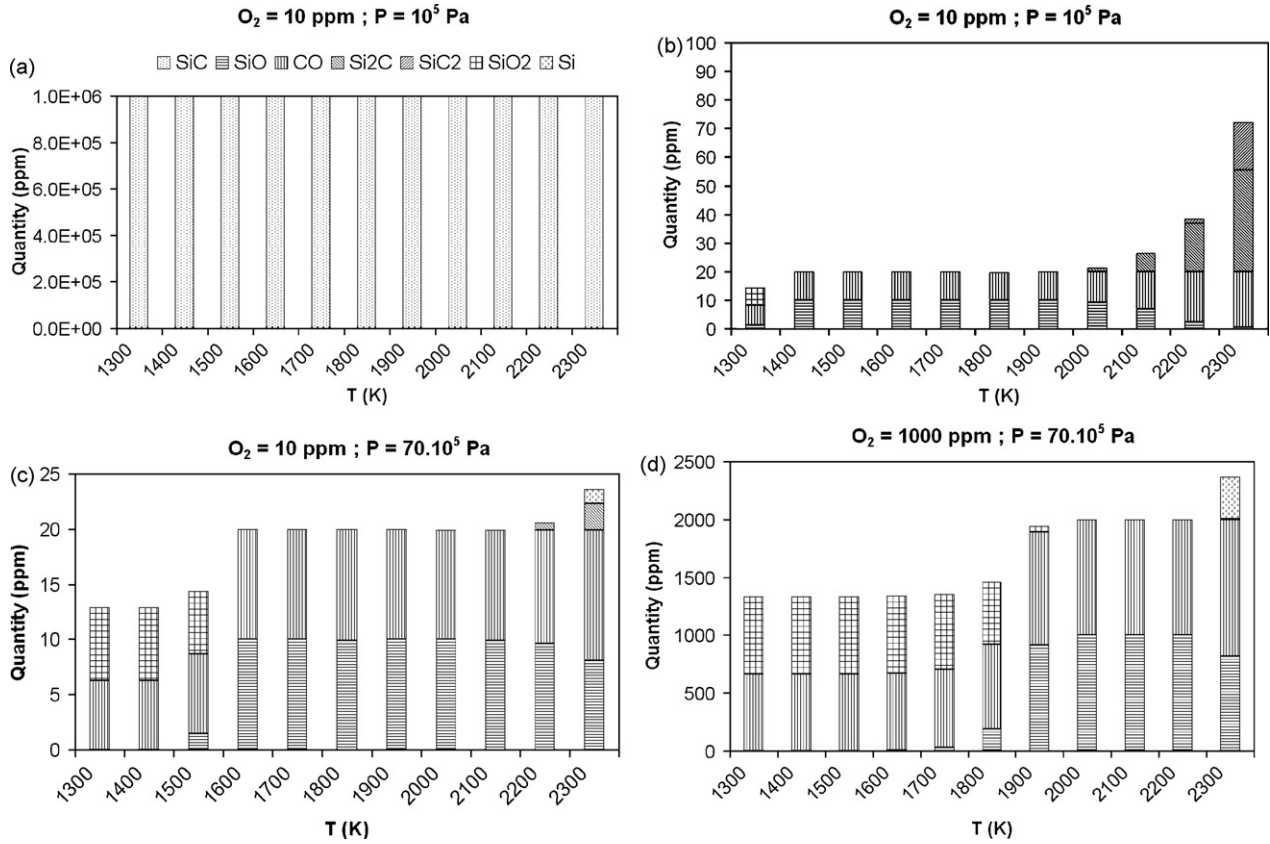


Fig. 1. Quantity of reactant and products versus temperature level for the numerical results obtained with the GEMINI code for SiC oxidation in different conditions: (a) and (b) He + 10 ppm O₂, $P_T = 10^5$ Pa; (c) He + 10 ppm O₂, $P_T = 7 \text{ MPa}$; (d) He + 1000 ppm O₂, $P_T = 7 \text{ MPa}$.

vapor is the oxidizing species (1800 instead of 1900 K). Moreover, water vapor is known to enhance SiC oxidation, without necessarily favoring its passivation, by not always forming a homogeneous oxide layer. This phenomenon is mainly due to the loss of the reaction products, and particularly H₂. When the oxidizing atmosphere is composed of 50% water vapor and 50% oxygen, the quantities of SiC consumed and SiO₂ produced are the average of the values obtained when pure H₂O or pure O₂ are the only oxidants. The silica is stable up to 1800 K, as with water vapor only. Thermodynamically, the reaction between SiC and H₂O occurs at lower temperatures than the reaction with O₂.

3. Analytical model

Wagner's model^{2,3} was used taking into account the solid species (SiC, SiO₂) and the major gaseous species present in the high temperature range (He, O₂, SiO, CO) at the transition for comparison to the numerical model. This model takes into account the mass-transfer constraints (open system) and leads to an analytical determination of the passive to active transition point in terms of oxygen partial pressure in the bulk gas for each temperature.

For each phase (solid and gaseous), the mass balance was established for each atomic compound and then the interface mass conservation (steady state) condition was imposed. The flux density J_i of the compound i at the interface was expressed using Fick's law:

$$J_i = \frac{-D_i(P_i^\infty - P_i^w)}{\delta_i RT} \quad (8)$$

where D_i the mass transfer coefficient of i in the carrier gas He, $D_i = D_{i,He}$, δ_i the thickness of the boundary concentration layer, R the ideal gas constant, T the temperature, P_i^∞ the partial pressure of the species i in the bulk gas, and P_i^w is the partial pressure at the interface. So, the fluxes of the species in the gaseous (G) phase are described by:

$$J_{O_2}^G + J_{SiO}^G = 0 \quad \text{and} \quad J_{He}^G = 0 \quad (9)$$

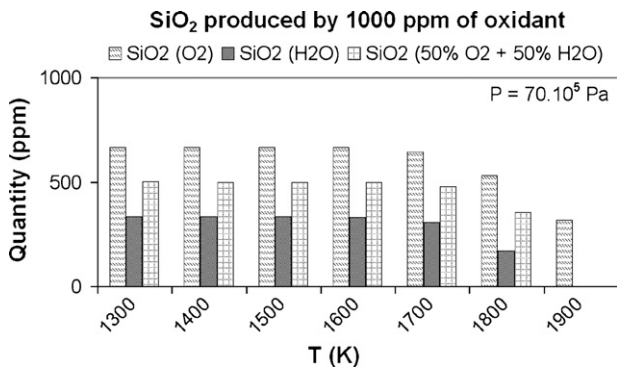


Fig. 2. Comparative results obtained with the GEMINI code for the oxidation of SiC under He plus O₂ or H₂O and their mixing (50% O₂ + 50% H₂O).

Table 1

Data used for the calculation of the diffusion coefficient of SiO, CO and O₂ in helium

<i>i</i>	σ_i (nm)	$\sigma_{i,He}$ (nm)	$D_{i,He}$ (cm ² s ⁻¹)
SiO	0.478	0.368	6.54
CO	0.359	0.308	9.34
O ₂	0.343	0.300	9.77

With $\sigma_{He} = 0.258$ nm.

With the two assumptions: $P_{O_2}^w = 0$ (interface consumption) and $P_{SiO}^\infty = 0$ (boundary layer concentration) and according to the Wagner approximation² for the ratio of the thicknesses (for a laminar flow), we obtain:

$$P_{O_2}^\infty = \left(\frac{D_{SiO}}{D_{O_2}} \right)^{1/2} \cdot P_{SiO}^w \quad (10)$$

The oxygen partial pressure can be expressed in terms of thermodynamic parameters accounting for the equilibria (1) and (2) with the two constants K_1 and K_2 defined by:

$$K_1 = \exp \left(- \frac{\Delta G_1^\circ}{RT} \right) = P_{SiO}^w \cdot \frac{P_{CO}^w}{P_{O_2}^w} \quad (11)$$

$$K_2 = \exp \left(- \frac{\Delta G_2^\circ}{RT} \right) = P_{CO}^w \cdot (P_{O_2}^w)^{-3/2} \quad (12)$$

Finally, the oxygen partial pressure of transition in the bulk is:

$$P_{O_2}^\infty = \left(\frac{D_{SiO}}{D_{O_2}} \right)^{3/8} \left(\frac{D_{CO}}{D_{O_2}} \right)^{1/8} K_1^{3/4} K_2^{-1/2} \quad (13)$$

In the case of an ideal gas at low density, the diffusion coefficient can be approximated using Chapman–Enskog theory.¹⁸ Data from the JANAF tables¹⁹ were used to calculate equilibrium constants. Table 1 gives the values of the diffusion coefficients used in this calculation and Table 2 presents the temperature and oxygen partial pressure data for the transitions.

Finally, the maximal oxygen partial pressure for the transition in helium is equal to:

$$P_{O_2}^\infty = 0.846 K_1^{3/4} K_2^{-1/2} \quad (14)$$

Fig. 3 shows the calculated transition temperature for SiC under helium and O₂ and the results are compared with those previously obtained by Balat in air³ and with the numerical model previously presented using Gemini code. We can see that this new analytical calculation is in good agreement with the previous results and the discrepancy between air and helium in expression (14) is less than 20%. The numerical and analytical calculations in helium are similar; the Wagner model gives $P_{O_2}^\infty = 3 \times 10^{13} \exp(-42233/T)$ and the Gemini calculation

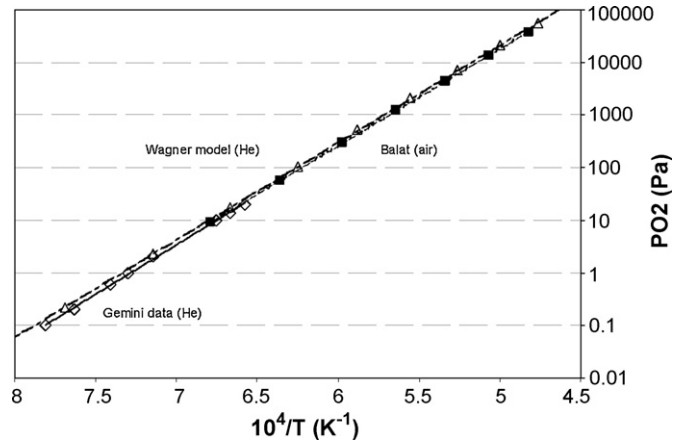


Fig. 3. Theoretical calculation for the active-to-passive transition for SiC – temperature versus oxygen partial pressure: black squares from Balat for air,⁴ white diamonds for this study using Gemini code and white triangles with dotted line for the modified Wagner model for helium.

$P_{O_2}^\infty = 5 \times 10^{13} \exp(-43292/T)$. The difference between the two curves tends to decrease when the temperature increases leading to a difference in the oxygen partial pressure of only 0.6% at 2100 K.

4. Experimental procedure

Two different silicon carbides provided by CEA Cadarache were studied. The first one was α -SiC from Saint-Gobain. It was densified by pressureless sintering performed above 2300 K and contained boron as major impurity. The second one was β -SiC, provided by Rohm and Haas, and produced by chemical vapor deposition. The samples were examined by X-ray diffraction to determine the different crystalline phases. α -SiC had a hexagonal structure (31–1232 ref. pattern) and the 2θ peak observed at 26.5° was characteristic of graphite (75–2078 ref. pattern). The β -SiC had a cubic structure (74–2307 ref. pattern) and seemed to be purer than the sintered α -SiC, based on the absence of the graphite peak.

The experimental set-up used is called MESOX (Moyen d'Essai Solaire d'Oxydation) and has been described elsewhere in details.^{3,4} It allows the heating of samples up to 2500 K, using a solar radiation concentrator, and can be operated at total pressures between 10^{-2} and 10^5 Pa. The device is composed of a sample-holder inside a cylindrical quartz vessel. The set-up is placed at the focus of a 6 kW solar furnace, thus elevated temperatures can be produced on materials such as SiC. A regulator, a gauge and a vacuum pump are used in order to precisely control the pressure during the experiment. A monochromatic (5 μ m) optical pyrometer is used to measure the temperature of the sample. The spectral (5 μ m) normal emissivity for SiC was

Table 2

Temperature and oxygen partial pressure for the active-to-passive transition in the oxidation of SiC in helium calculated with the modified Wagner model

<i>T</i> (K)	1200	1300	1400	1500	1600	1700	1800	1900	2000	2100	2200	2300
$P_{O_2}^\infty$	0.01	0.22	2.3	17.7	105	525	2077	7065	21132	56626	138040	309987

Table 3

Total pressure and temperature conditions, oxidation regime and relative mass variation for α - and β -SiC samples tested under helium

Samples	T (K)	P (10^4 Pa)	Oxidation	$\Delta m/m$ (%)
α -SiC A	1330	7.03	Passive	0.012
α -SiC C	1600	7.04	Passive	-0.027
α -SiC B	1610	6.60	Passive	0.270
α -SiC G	2000	6.54	Active	-1.460
β -SiC 7	1360	6.70	Passive	-0.025
β -SiC 8	1540	6.71	Passive	-0.042
β -SiC 3	1670	6.54	Active	-0.024
β -SiC 4	1650	6.80	Active	-0.084
β -SiC 6	1970	6.85	Active	-0.340

Table 4

Total pressure and temperature conditions, oxidation regime and relative mass variation for α - and β -SiC samples tested under helium + 1000 ppm oxygen N48

Samples	T (K)	P (10^4 Pa)	Oxidation	$\Delta m/m$ (%)
α -SiC F	1600	6.75	Passive	-0.016
α -SiC H	1970	6.57	Active	-0.810
β -SiC 1	1680	6.72	Passive	-0.014
β -SiC 5	1940	6.71	Active	-0.400

measured in our laboratory using a direct method²⁰ and the value is 0.90.

The test parameters were chosen to reproduce the nominal, incidental and accident conditions of use of the GFR, within the limit of the MESOX set-up.

The tests were conducted around 1300, 1600 and 2000 K. The gradual opening of a shutter placed between the sample and the solar concentrator allowed for control of the temperature. Oxidation experiments were conducted at constant surface temperature during 600 s after rapidly (few seconds) heating to the test temperature. Then, specimens were cooled by closing the shutter, which isolated the specimen from the heat source.

It was impossible to reproduce the predicted conditions of the future nuclear reactor, that is to say 7 MPa; so the tests were conducted near atmospheric pressure (7×10^4 Pa), the solar furnace being at 1500 m altitude) under a gas flow of $1.7 \times 10^{-4} \text{ m}^3 \text{ s}^{-1}$ (101 min^{-1}), controlled by a pumping system.

The atmosphere for the tests was helium (Air Liquide, grade U) which contained roughly, according to the supplier, 20 ppm oxygen and 5 ppm water. To simulate higher levels of impurities, 1000 ppm of oxygen (Air Liquide N48) was added to the helium during some experiments.

After oxidation, three analytical methods were used to characterize the oxidation products. First, the samples were weighed to detect mass changes. Then, the surfaces of the samples were analyzed by using X-ray Photoelectron Spectroscopy (XPS). The Si 2p, O 1s and C 1s photoelectron lines were studied. Scanning Electron Microscopy (SEM) was also used to observe

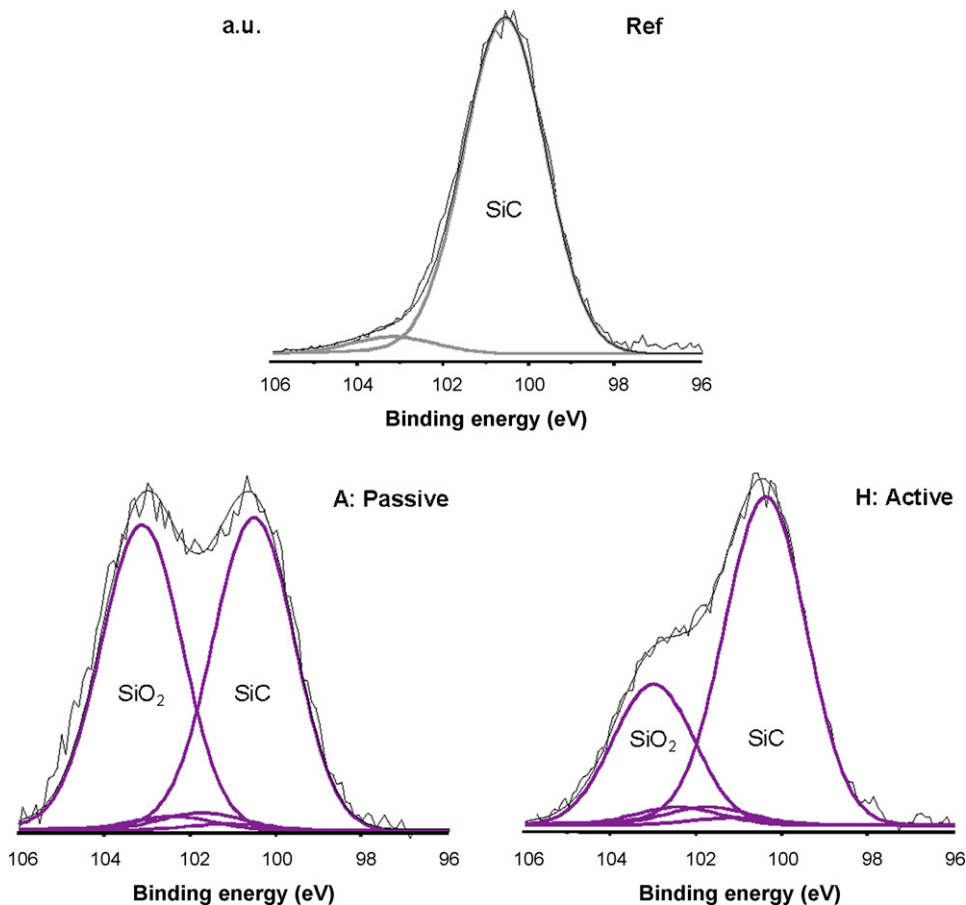


Fig. 4. Si2p photoelectron peaks collected on α -SiC samples (ref.) and after passive (left, sample A) and active (right, sample H) oxidation conditions.

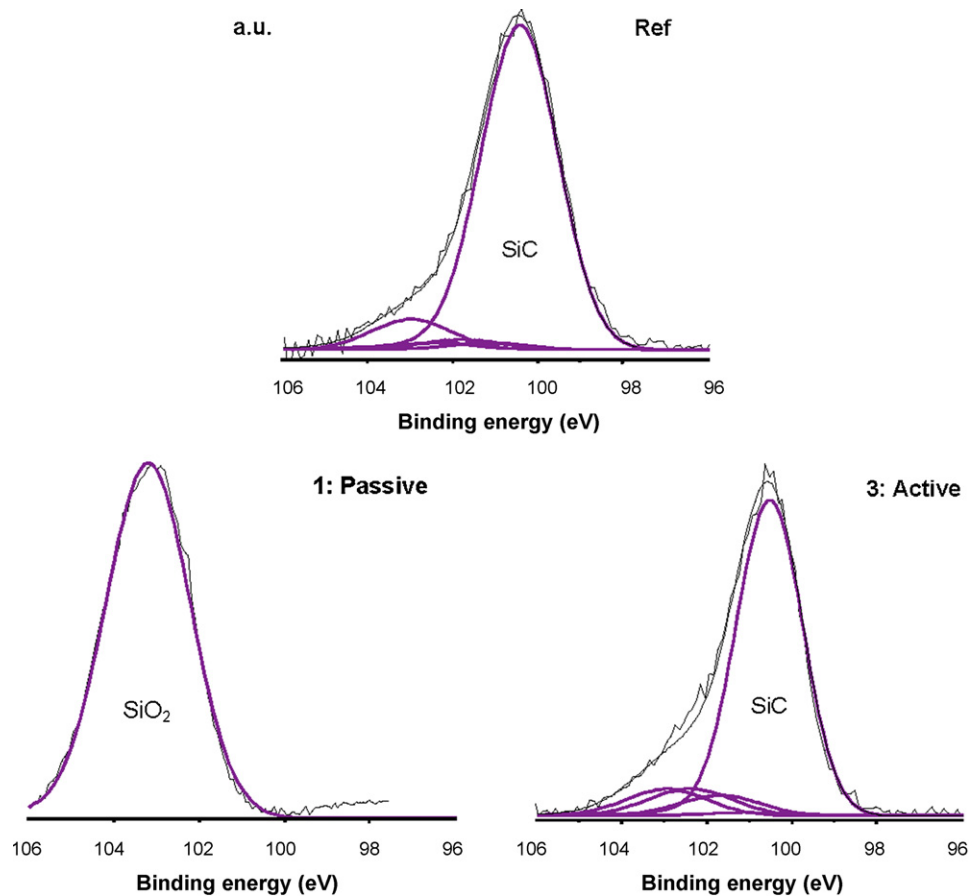


Fig. 5. Si2p photoelectron peaks collected on β -SiC samples (ref.) and after passive (left, sample 1) and active (right, sample 3) oxidation conditions.

the surface morphology of the materials before and after oxidation.

Tables 3 and 4 summarize the results of the different experiments carried out during this study under helium and under helium with oxygen. The temperature and the total pressure, the oxidation regime and the relative mass variation of the samples are reported. Some representative XPS spectra and SEM micrographs of α -SiC and β -SiC as-received and after various oxidation treatments are also displayed. After testing, α -SiC samples were analyzed by XRD to detect structural modifications. Except for the low intensity carbon peak, no change was observed after oxidation. Carbon should react with oxygen contained in helium during testing. SiO_2 cannot be observed by XRD because of its amorphous structure. For β -SiC samples, no change was detected.

The following results were deduced from the coupled interpretations of XPS and SEM analyses and relative mass variation data.

XPS analysis (SIA 200 RIBER CAMECA UHV) used Al K α radiation with an energy of 1486.6 eV. Kinetic energies of the photoelectrons were measured with a two-stage RIBER CAMECA MAC 2 spectrometer. The analyzer resolution was 1 eV. An Ar⁺ ion gun (RIBER CAMECA C.I. 50) was used to sputter clean specimen surfaces. The ion energy was set to 1 keV and the sputtering time was 10 min. The photoelectron spectra were calibrated using the C 1s signal detected at a binding

energy of 285 eV from adventitious carbon. Atomic compositions were calculated with the corrected Scofield coefficients²¹ of the transmission function of the analyzer and/or with experimental coefficients determined for a reference compound. The continuum spectrum was subtracted according to the Shirley method.²²

Si 2p photoelectron peaks were collected for α -SiC (Fig. 4) and β -SiC (Fig. 5). For each material, graphs of a reference sample and oxidized (active and passive) samples are displayed. The Si 2p lines were fitted into two main Gaussian components at 100.5 and 103.2 eV that were attributed to Si–C and Si–O bonds, respectively. The SiC component at 100.5 eV was predominant when the oxidation was active. In the case of passive oxidation, the 103.2 eV peak, typical of SiO_2 , was at least equivalent to the SiC component. Intermediary detected components were due to possible silica reduction by argon ion bombardment during sputtering. Even for active oxidation, silica was sometimes detected. This can be explained by the fact that under oxidizing atmosphere, a SiO_2 layer is always formed at lower temperature, during the cooling of the sample after the temperature plateau.

SEM micrographs of various α - and β -SiC samples are shown on Figs. 6 and 7. For each material, a reference sample and four samples that have undergone oxidation under helium (samples B and G; samples 3 and 7) and under helium with 1000 ppm oxygen (samples F and H; samples 1 and 5) are displayed. For α -SiC (Fig. 6) under helium, when the oxidation regime was

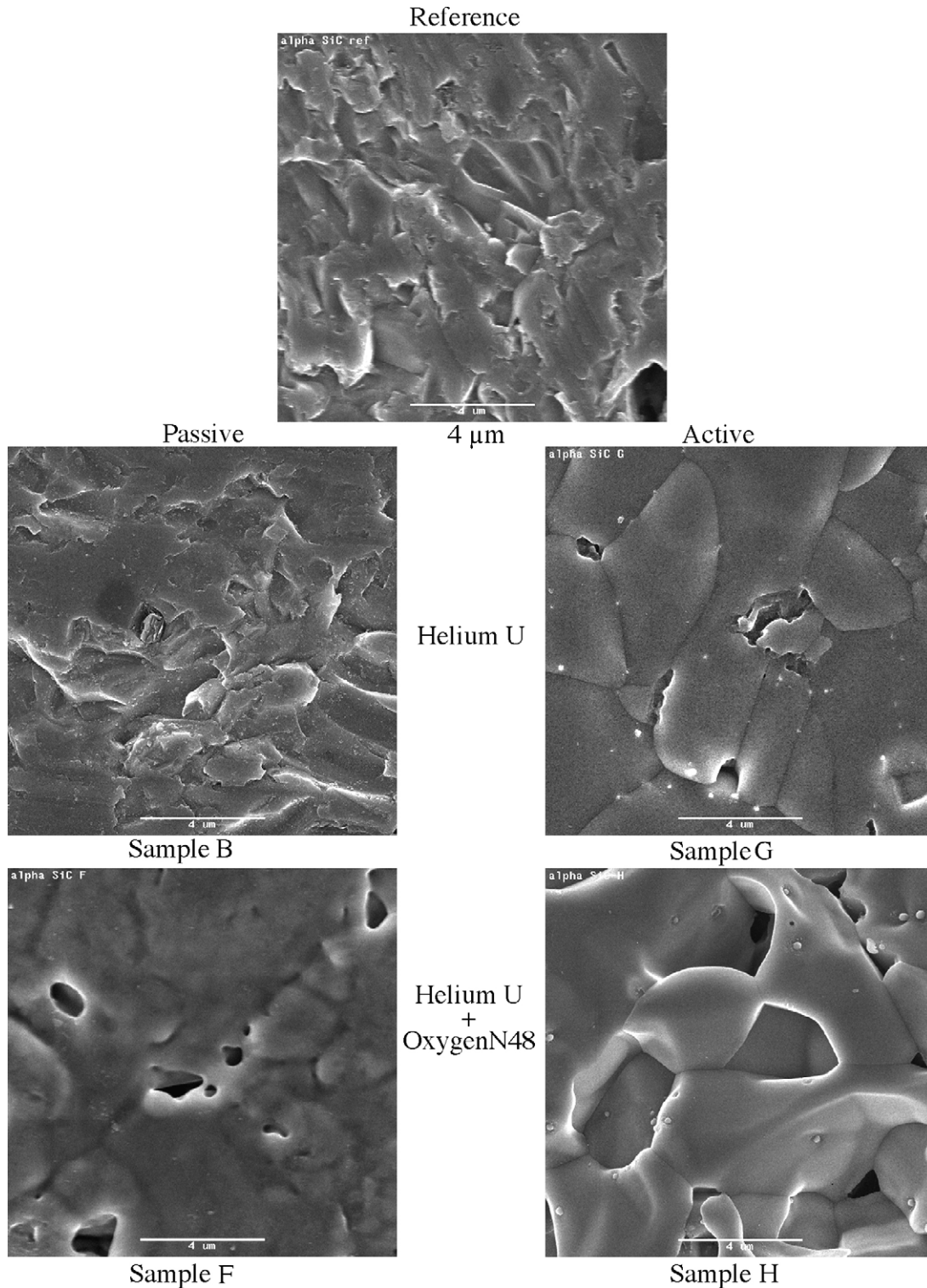


Fig. 6. SEM micrographs of α -SiC (ref. is the top image) and after passive (left, samples B and F) and active (right, samples G and H) oxidation conditions (upper images in He; lower images in He + 1000 ppm O_2). The samples are the following as mentioned on the image: B, G, F and H (see conditions in Tables 3 and 4).

passive, the morphology of sample B was nearly identical to the reference; however a thin silica layer was present as revealed by XPS and mass gain. For an active oxidation regime (sample G), vaporization of SiC occurred, porosity appeared and a larger mass loss was measured. Under helium with 1000 ppm oxygen, a smooth silica layer was formed on the sample surface when

the oxidation was passive (sample F). During active oxidation, the vaporization of the material was evident, and a very thin silica layer was produced during cooling on the eroded material surface (sample H). For β -SiC (Fig. 7), under helium, a passive oxidation regime did not affect the sample morphology and a thin silica layer appeared (sample 7). During active oxidation,

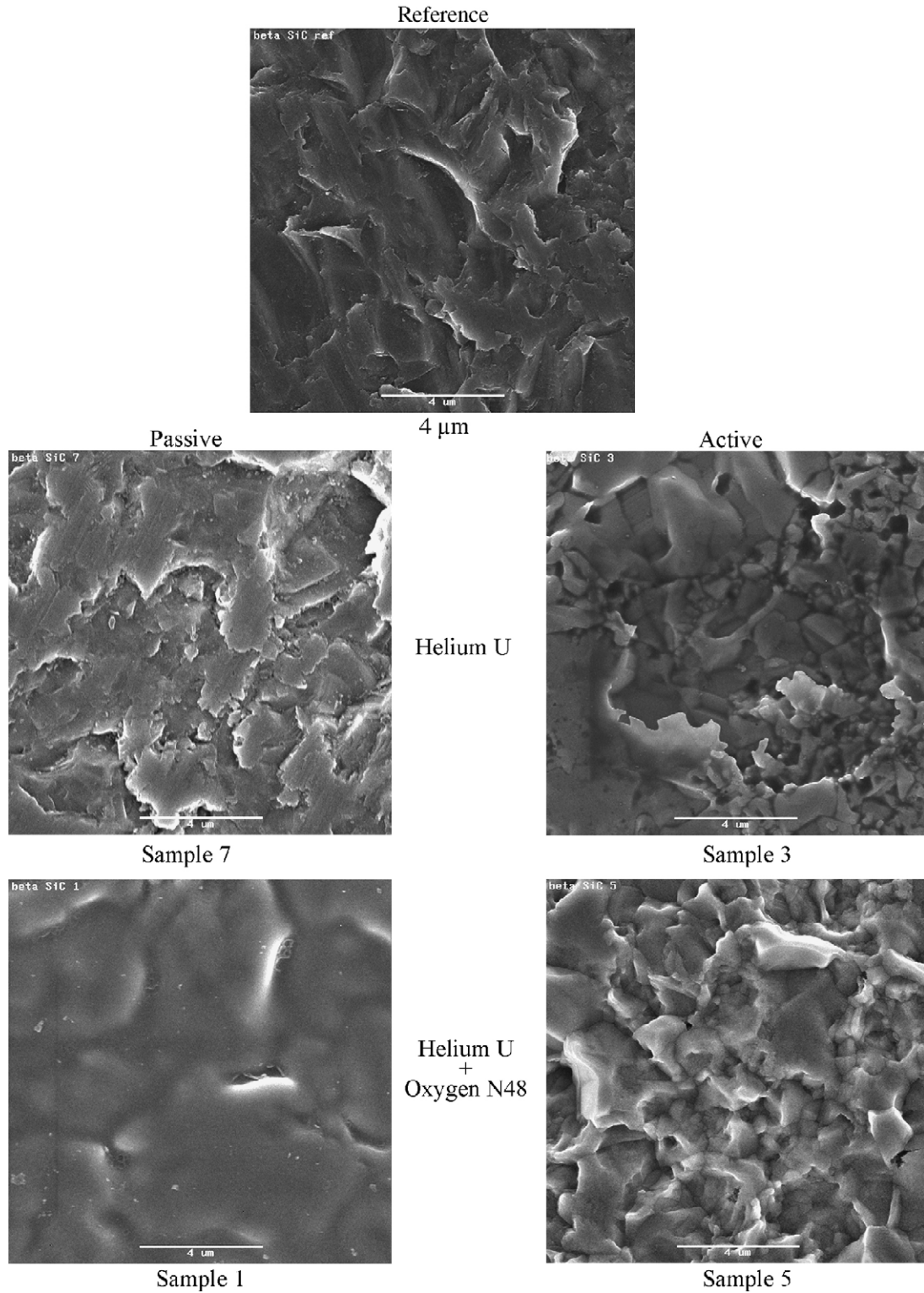


Fig. 7. SEM micrographs of β -SiC (ref. is the top image) and after passive (left, samples 7 and 1) and active (right, samples 3 and 5) oxidation conditions (upper images in He; lower images in He + 1000 ppm O_2). The samples are the following as mentioned on the image: 7, 3, 1 and 5 (see conditions in Tables 3 and 4).

the sample surface became sharp and damaged, with cavities formed (sample 3). When 1000 ppm oxygen was added to the helium, a smooth and homogeneous silica layer was formed on the surface for passive conditions (sample 1). In contrast, for active oxidation, the sample surface was altered and a very thin

oxide layer formed only during cooling, as revealed by XPS (sample 5).

According to the experimental results, the crystallographic structure of the SiC influences its physico-chemical behavior. First of all, the temperature of the passive to active transition was

higher for α -SiC. It happened in the range of 1600–1970 K (for the two gas compositions) and it was between 1540 and 1650 K for β -SiC under helium and between 1680 and 1940 K under helium with 1000 ppm oxygen added (Tables 3 and 4). A study is in progress to obtain more accurate transition temperatures. Concerning the structural integrity of the material during active oxidation, β -SiC seems better, according to the sample mass loss. Around 2000 K and under oxidizing atmosphere (1000 ppm O_2), the mass loss of the α -SiC was twice the β -SiC mass loss, and four times higher under helium with low oxygen partial pressure (Table 4).

Experimentally it was observed that the level of oxidizing species had an impact on the physico-chemical behavior of SiC as was also predicted by thermodynamic calculation. At 1600 K, for α -SiC, the addition or not of oxygen did not change the oxidation regime that remained passive. However, a lesser mass loss was noted when more oxygen was present. Moreover, the passive to active transition was lower for β -SiC, with no change in mass loss. At 2000 K, the increase of the oxygen content did not affect the passive to active transition for either α - and β -SiC, as all samples underwent active oxidation. For the mass loss, the crystallographic structure was an important factor. Whatever the oxygen partial pressure in the surrounding atmosphere, mass loss was nearly the same for β -SiC. On the contrary, α -SiC mass loss was about 50% lower for the higher oxygen partial pressure.

5. Conclusion

Silicon carbide is a promising structural material for Generation IV nuclear reactors. Because of its mechanical and physico-chemical properties, it maintains structural integrity at high temperature in a helium environment. However, it is necessary to evaluate its oxidation resistance in not only nominal conditions but also in incidental or accidental ones.

The numerical study presented indicated that SiC has promise as a structural material of the future reactors. At atmospheric pressure and in the nominal temperature range (1300–1500 K), SiC forms a protective silica layer at oxygen levels of 100 ppm and higher. However, if the pressure is elevated to 7 MPa, only 10 ppm of oxygen is needed to be in the passive domain. Moreover, with 1000 ppm, SiO_2 is present up to 1900 K, temperature predicted for incidental conditions.

The experimental study has evaluated the physico-chemical behavior of SiC at high temperature at atmospheric pressure. At the nominal temperature of use, 1300 K, both of α and β -SiC can be used. Differences in behavior were observed around 1600 K, with α -SiC having a higher temperature for its passive to active oxidation transition. Under incidental temperature conditions that is to say about 1900 K, both α and β -SiC underwent active

oxidation. However, the mass loss for β -SiC was lower than for α -SiC. For higher oxygen levels, the oxidation depended on the crystallographic structure. α -SiC had a higher temperature for its passive to active transition, but a lower mass loss.

References

1. Les réacteurs nucléaires à caloporteur gaz, *Monographies DEN*. CEA Saclay, Editions du Moniteur, Octobre 2006.
2. Wagner, C., Passivity during the oxidation of silicon at elevated temperature. *J. Appl. Phys.*, 1958, **29**, 1295–1297.
3. Balat, M., Flamant, G., Male, G. and Pichelin, G., Active to passive transition in the oxidation of silicon carbide at high temperature and low pressure in molecular and atomic oxygen. *J. Mater. Sci.*, 1992, **27**, 697–703.
4. Balat, M. J. H., Determination of the active-to-passive transition in the oxidation of silicon carbide in standard and microwave-excited air. *J. Eur. Ceram. Soc.*, 1996, **16**, 55–62.
5. Presser, V. and Nickel, K. G., Silica on silicon carbide. *Crit. Rev. Solid State Mater. Sci.*, 2008, **33**, 1–99.
6. Ogura, Y. and Morimoto, T., Mass spectrometric study of oxidation of SiC in low-pressure oxygen. *J. Electrochem. Soc.*, 2002, **149**, 47–52.
7. Narushima, T., Goto, T., Hirai, T. and Iguchi, Y., High-temperature oxidation of silicon carbide and silicon nitride. *Mat. Trans. JIM*, 1997, **38**, 821–835.
8. Yin, X., Cheng, L., Zhang, L. and Xu, Y., Oxidation behaviors of C/SiC in the oxidizing environments containing water vapor. *Mater. Sci. Eng. A*, 2003, **348**, 47–53.
9. Jacobson, N. S., Fox, D. S. and Opila, E. J., High temperature oxidation of ceramic matrix composites. *Pure Appl. Chem.*, 1998, **70**, 493–500.
10. Opila, E. J. and Hann, R. E., Paralineer oxidation of CVD SiC in water vapor. *J. Am. Ceram. Soc.*, 1997, **80**, 197–205.
11. Opila, E. J., Variation of the oxidation rate of silicon carbide with water–vapor pressure. *J. Am. Ceram. Soc.*, 1999, **82**, 625–636.
12. More, K. L., Tortorelli, P. F., Ferber, M. K. and Keiser, J. R., Observations of accelerated silicon carbide recession by oxidation at high water–vapor pressures. *J. Am. Ceram. Soc.*, 2000, **83**, 211–213.
13. Tortorelli, P. F. and More, K. L., Effects of high water–vapor pressure on oxidation of SiC at 1200 °C. *J. Am. Ceram. Soc.*, 2003, **86**, 1249–1255.
14. Opila, E. J., Fox, D. S. and Jacobson, N. S., Mass spectrometric identification of Si–O–H(g) species from the reaction of silica with water vapor at atmospheric pressure. *J. Am. Ceram. Soc.*, 1997, **80**, 1009–1012.
15. Perez, F. J. and Ghoniem, N. M., Chemical compatibility of SiC composite structures with fusion reactor helium coolant at high temperatures. *Fusion Eng. Des.*, 1993, **22**, 415–426.
16. Balat, M., Berjoan, R., Pichelin, G. and Rochman, D., High temperature oxidation of sintered silicon carbide under pure CO_2 at low pressure: active–passive transition. *Appl. Surf. Sci.*, 1998, **133**, 115–123.
17. Thermodata, Saint Martin d’Heres, France.
18. Bird, R. D., Steward, W. E. and Lightfoot, E. N., *Transport Phenomena*. J Wiley & Sons, NY, 1960.
19. Chase M. W. and Davies J. R., *JANAF Thermodynamical Tables*, 3rd ed., *J. Phys. Chem. Ref. Data*, vol. 14 (Suppl. 1), 1985.
20. Balat-Pichelin, M., Robert, J. F. and Sans, J. L., Emissivity measurements on carbon-carbon composites at high temperature under high vacuum. *Appl. Surf. Sci.*, 2006, **253**, 778–783.
21. Scofield, J. H., Hartree-Slater subshell photoionization cross-sections at 1254 and 1487 eV. *J. Elect. Spect. Relat. Phenom.*, 1976, **8**, 129–137.
22. Shirley, D. A., High-resolution X-ray photoemission spectrum of the valence bands of gold. *Phys. Rev. B*, 1972, **5**, 4709–4714.